MODELING OF STRUCTURES SUBJECTED TO WIND GENERATED WAVES

by

Erich J. Plate and John H. Nath

CER67-68EJP-JN68

11th Conf. on Coastal Engr. - London 1968

MODELING OF STRUCTURES SUBJECTED TO WIND GENERATED WAVES

by

Erich J. Plate* and John H. Nath*

ABSTRACT

The difficulties inherent in the direct determination of loads on off-shore structures which are exposed simultaneously to wind and waves make it desirable to model each situation in the laboratory. It is shown here that scaling of the loads and the waves is possible by using waves which are generated by blowing air over the surface of a laboratory channel, and by choosing a model material with an appropriate modulus of elasticity. Wind-generated waves such as those measured in the wind water tunnel of Colorado State University have a dimensionless spectrum (Hidy and Plate (1965)) that is identical in shape to that found off the coast of Florida under hurricane conditions (Collins (1966)). Furthermore, it has been shown that hydro-elastic modeling is quite feasible (LeMehaute (1966)). These two results are combined to give modeling criteria for off-shore structures if direct wind forces are disregarded.

Some consideration is also given to dynamic wind load modeling and to the question whether simultaneous modeling of both the wave and the wind forces is possible in a laboratory. In principle, this appears feasible, but for sufficiently large scale models, fetch lengths may be required which are larger than typical laboratory channels.

CER67-68EJP-JN68
also CEP67-68 EJP-JN101
and CEP68-69 EJP34

*Civil Engineering Department, Colorado State University

MODELING OF STRUCTURES SUBJECTED TO WIND GENERATED WAVES

INTRODUCTION

The increased use of off-shore structures for the exploration and exploitation of the oceans has created a demand for accurate design information on the load conditions to which the structures are subjected. In contrast to most land based structures, the critical load conditions for an off-shore structure may be dynamic in nature and induced by the water surface waves, so that analytical design procedures may become very complicated except for simply shaped structural elements.

Present analytical procedures for determining the response even of simple structures to periodic waves are not exact. For example, it is customary to use the Morrison equation to determine the wave forces acting on a vertical cylinder. In the Morrison equation, the inertia and drag coefficients must be determined experimentally. In some cases these coefficients can only be described statistically. Furthermore, they may vary with depth, as has recently been demonstrated by Pierson and Holmes (1965).

Under these circumstances it becomes desirable to study the dynamic behavior of a structure on a laboratory scale, which is quite feasible as will be shown in this paper. LeMehaute (1966) has shown that hydro-elastic modeling can be accomplished conveniently by using modern plastics for model construction. If it can be ascertained that the response of the structure is linear, then the modeling problem consists of requiring identical shapes of transfer functions in model and prototype obtained by the modeling transformation. The transfer function is then the quantity which needs to be determined from the experiment, and it can be found conveniently by exciting the model structure with a sequence of sine waves, and finding the response to each of them.

Most structural responses are nonlinear (although many are nearly linear), so that their transfer functions cannot be constructed by superposition. In such cases laboratory experiments are the only alternatives to potentially extremely complex calculations, for which the model structure must be excited with a forcing function which is dynamically similar to the prototype forcing function. In particular, for structures excited by wind generated waves, the model wave spectrum must be dynamically similar to that of the prototype. Dynamic similarity of the spectrum does imply similarity of the shape of the spectra, as well as similarity of the energy contained in the spectra.

The need for similarity in spectral shape has been realized for some time. Thus, Nath and Harleman (1967) produced a spectrum whose shape was similar to that of spectra found in parts of the Atlantic

Ocean by Pierson and Moskowitz (1964). They used a wave generator for exciting model structures which was programmed to generate a quasi-random wave train with a spectrum of the desired shape.

Wave trains produced by a wave generator have several features which differ from that of a wind generated wave pattern. A wave generator can only produce wave components which agree with the free modes of the water surface. That is, each of the wave components is sinusoidal in shape and travels independently of all other wave components. Thus, when a large wave is formed by the superposition of component sinusoidal waves that are momentarily in phase, although of different wave lengths, one finds that the life of the wave is fairly short. The large wave forms when the components are in phase, and then disappears as the components become out of phase due to the different component celerities. In contrast to this, one finds that large wind generated waves at high wind speed are quite long-lived and are, therefore, not composed of independently traveling sinusoidal waves. Nor is their total shape sinusoidal. In Fig. 1 an example is shown of a significant wave which is found at a wind speed of approximately 10 m/sec. This wave has been obtained by averaging the highest 20 waves from a record of about 300 waves measured in a laboratory channel. The waves were superimposed in such a way that their highest points coincided on the time axis and the ordinate values were averaged. A confidence band given by the local standard deviations of the coordinate values about the mean is also shown. It is apparent that even though the wave travels as a whole, its shape is definitely not sinusoidal. Consequently, even though the spectrum of generator produced random waves might match that of wind generated waves, the shapes of the resulting individual waves are not exactly the same. Results obtained by this procedure are therefore subject to question, particularly if the dynamic response of the structure is nonlinear.

A second, and possibly more important difference between a generator produced spectrum and a fully developed wind wave spectrum lies in the inability of the former to properly model the magnitudes of the spectral densities. Complete dynamic modeling requires that both wave lengths and amplitudes are modeled by the same scale factor. As shall be shown later, this condition requires that the dominant wave, which corresponds to the frequency at the peak in the spectrum for fully developed conditions, reaches its maximum possible amplitude. It is doubtful that this condition can be met while maintaining the required spectral shape, because the variance of a wave spectrum driven by strong winds increases with fetch, while that of the paddle generated wave spectrum decreases, partly due to viscosity, and partly due to breaking when superposition of component waves increases wave amplitudes beyond their stability limit.

More suitable test conditions are obtained when wave trains are used, whose spectra, as well as shape and amplitudes of individual waves, resemble those of wind generated waves, but on a smaller scale. Such wave trains are found in the laboratory if air is blown over the surface of water standing in a channel. In this paper, the application of wind generated waves to modeling of wave forces is discussed. Since

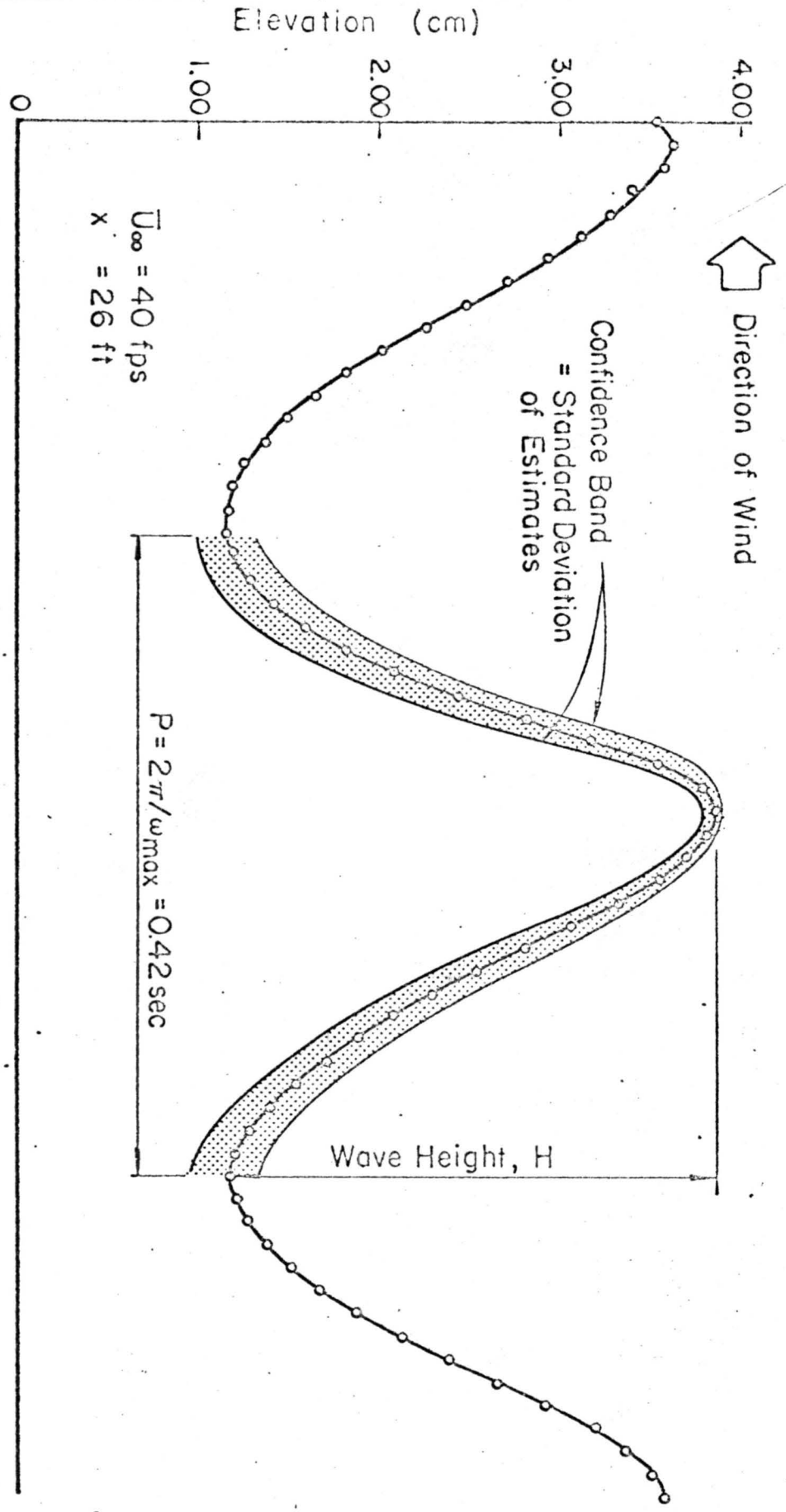

Fig. 1 Average wave form of wave at high wind velocity (from Po-Chang).

the wind generated laboratory waves have fewer drawbacks than paddle generated waves, it would be advisable to use them to obtain the load conditions on model structures. By this method one also obtains a means to evaluate the wind loads on the part of the structure above the water surface.

As shall be discussed in the first part of this paper, the spectrum of fully developed wind generated waves in a laboratory is similar in shape to that found for ocean waves, and it also yields a relationship between peak frequency and variance of the spectrum which is scaled by the Froude number in such a way that no change in scale between vertical and horizontal dimensions becomes necessary. In the second part, considerations will be given to the modeling requirements of the structure. This will be discussed on the basis of simple linear structures, and it is shown that Cauchy number similarity is feasible together with Froude number similarity. Modeling of the air flow above the water for simultaneous scaling of wave forces and wind forces is discussed in the third part of this paper. It is realized that the wind forces might be affected by the amount of spray carried in the air and it is felt that it may be possible to model this phenomenon, although very little is known about this topic. Otherwise it appears that dynamic modeling, by Strouhal number, can be accomplished in conjunction with Froude and Cauchy number modeling, but the fetch lengths required might be prohibitive. This is illustrated in an example which forms the last part of the paper.

The Similarity Spectrum of Wind Generated Waves

The driving forces acting on the submerged portion of a dynamically loaded off-shore structure result from the wave field generated by the wind. They act in addition to the wind force on the superstructure. Even though this wave field usually appears random both in space and time, it is nevertheless possible to distinguish, especially in the neighborhood of coasts, crests of waves which give the wave field an appearance of local two-dimensionality, with a predominant direction of progression perpendicular, or almost perpendicular, to the crest. For such a wave pattern, a laboratory analogue exists in the wind generated waves which are obtained when air is blown over the surface of the channel in which water is standing. It seems possible that the majority of all wind driven ocean waves outside of a storm center consists basically of a dominant pattern of this kind. This would offer a logical explanation for the observation that one-dimensional wave spectra both in the laboratory and in oceans have an approximately equal shape. An illustration of this phenomenon is given in Fig. 2a where a typical laboratory spectrum, obtained by Hidy and Plate (1965), is compared with a set of ocean wave spectra generated by strong off-shore winds off the coast of Florida shortly after the passage of Hurricane Dora, in September 1964. The spectra were calculated by Collins (1966). The peak density of the larger ocean wave spectrum is 10,000 times larger than the peak density of the laboratory spectrum. Yet, the shapes do not differ significantly.

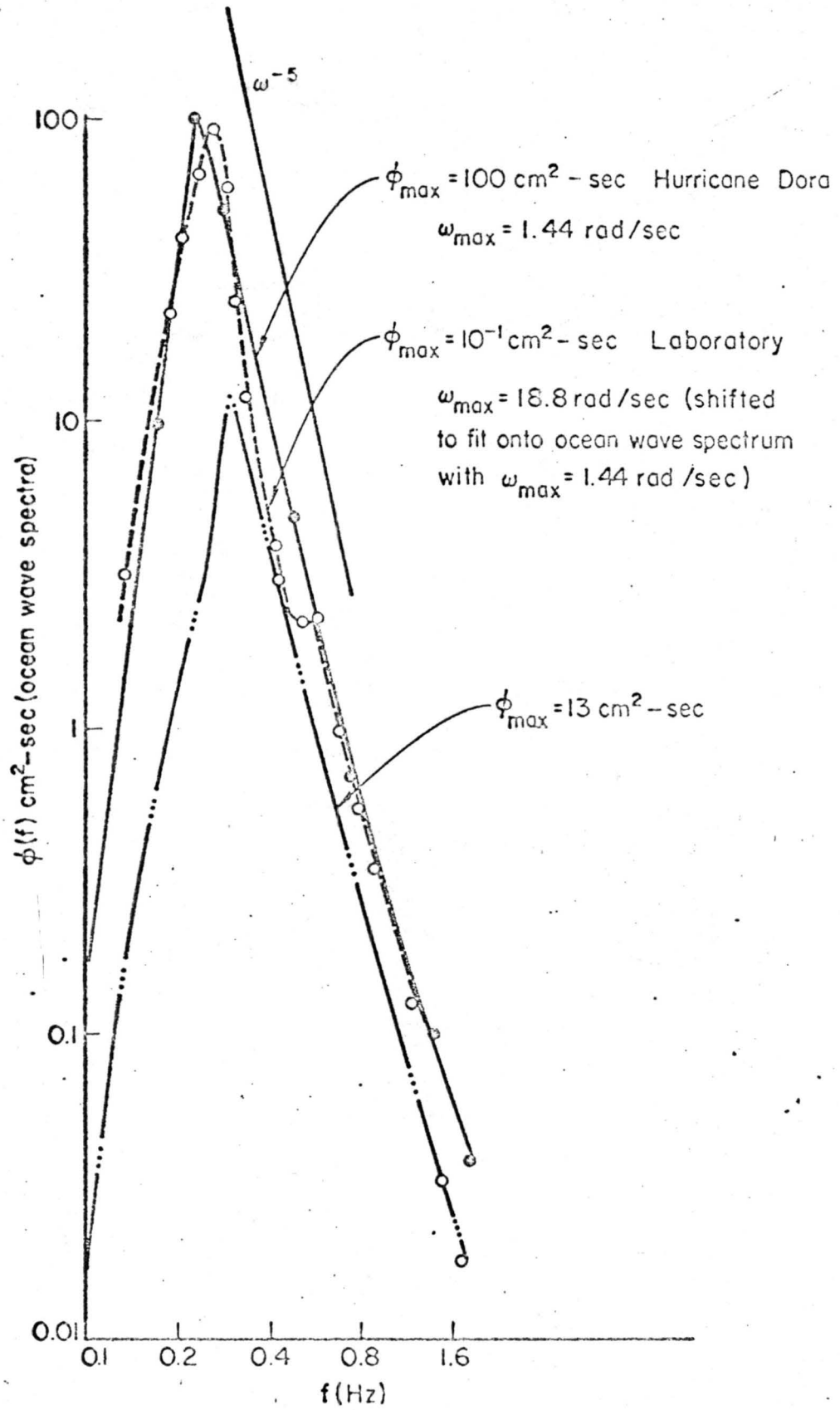

Fig. 2a Examples of Ocean and Laboratory Spectra

The identical shape of the dimensionless spectra shall be explored here. A non-dimensional form of the spectral shape that is suitable for the purpose of this paper has been suggested by Hidy and Plate (1965). Hidy and Plate (1965) recommended to non-dimensionalize the spectra by dividing the frequency axis by ω_{max}, which is the angular frequency at which the spectral peak $\phi(\omega_{max})$ is observed. The spectral density $\phi(\omega)$ was reduced so that the area under the non-dimensional spectrum $S(\omega/\omega_{max})$ is equal to 1. This leads immediately to the requirement

$$S\left(\frac{\omega}{\omega_{max}}\right) = \frac{\omega_{max}}{\sigma^2} \phi(\omega) \tag{1}$$

where σ^2 is the variance of the water surface elevation. This non-dimensionalizing procedure is equally valid for ocean wave data, as was shown by Colonell (1966). In Fig. 2b, the average curve of Hidy and Plate (1965) is given, which is representative for many different laboratory spectra. The similarity of this shape with that of Fig. 2a is noted. Also, it is seen that the high frequency end of the spectrum follows approximately a ω^{-5} law, as predicted by Phillips (1958). However, the -5 law seems to be only an approximation to the spectra at high frequencies. There is evidence that the exponent in the power law varies from about -7 near the spectral peak to -4 at higher frequencies.

More significant than the high frequency behavior of the individual spectrum is the fact that all spectra obtained from ocean or laboratory are bounded at the high frequency end by a universal curve given by the equation of Phillips

$$\phi(\omega \geq \omega_{max}) = 1.05 \quad 10^{-2} g^{+2} \omega^{-5} \tag{2}$$

where g is the constant of gravity. This is shown in Fig. 3, which has been reproduced from Hess (1968). Phillips (1958) derived Eq. 2 by using dimensional analysis. Recently Plate, Chang and Hidy (1968) have provided arguments which deduce the -5 power law as an upper limit of spectral growth, independent of the shape of the individual spectrum, provided only that all spectra are similar. The -5 power law then becomes a law which relates peak spectral density $\phi(\omega_{max})$ to ω_{max}. Since this law plays a key role in the modeling criteria to be developed, the derivation shall be outlined here.

The basic assumptions are:

a. The spectrum has a sharp peak near ω_{max}, and can be described by the similarity shape of Fig. 2b. According to Longuet-

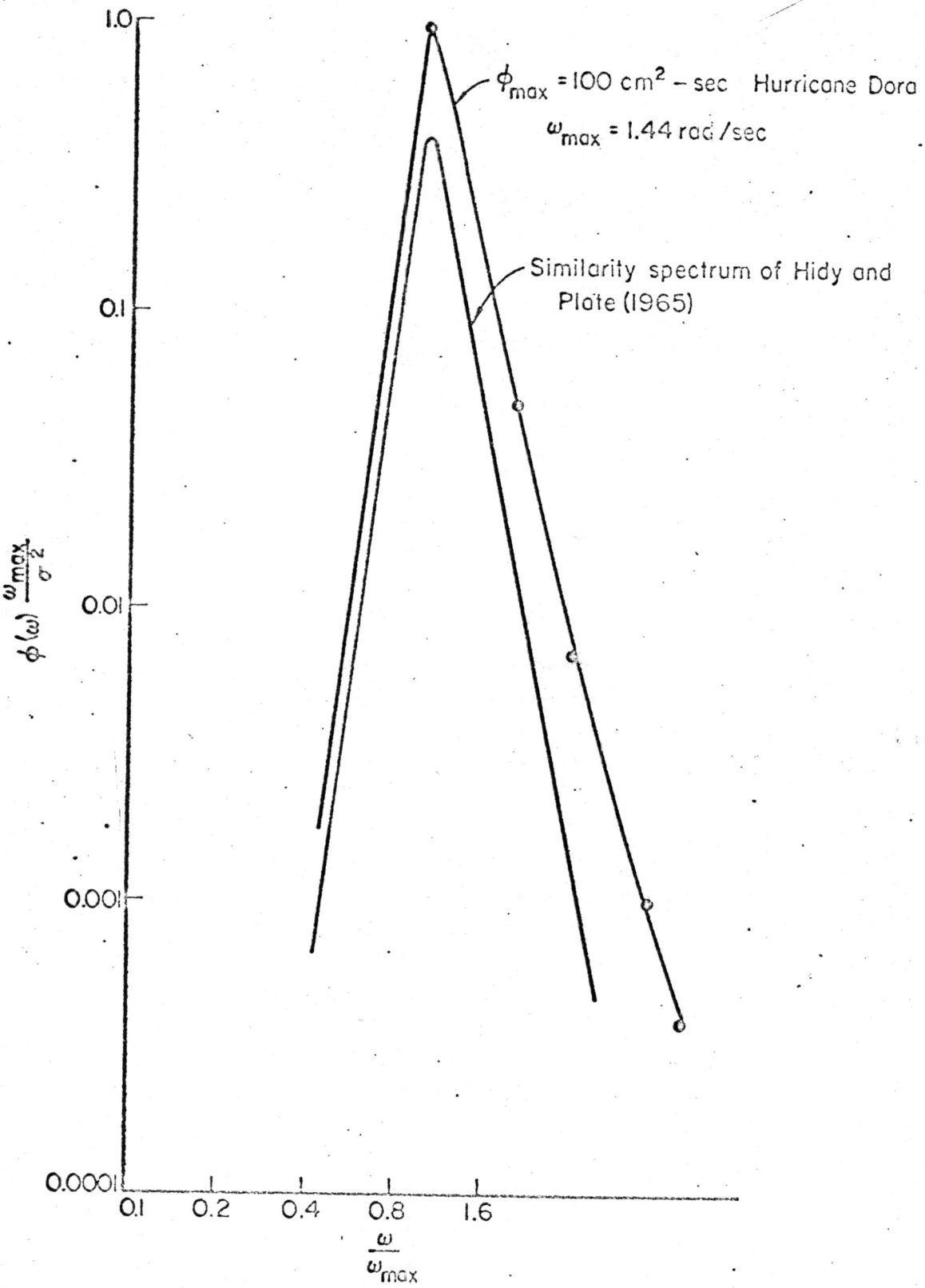

Fig. 2b Examples of Ocean and Laboratory Spectra

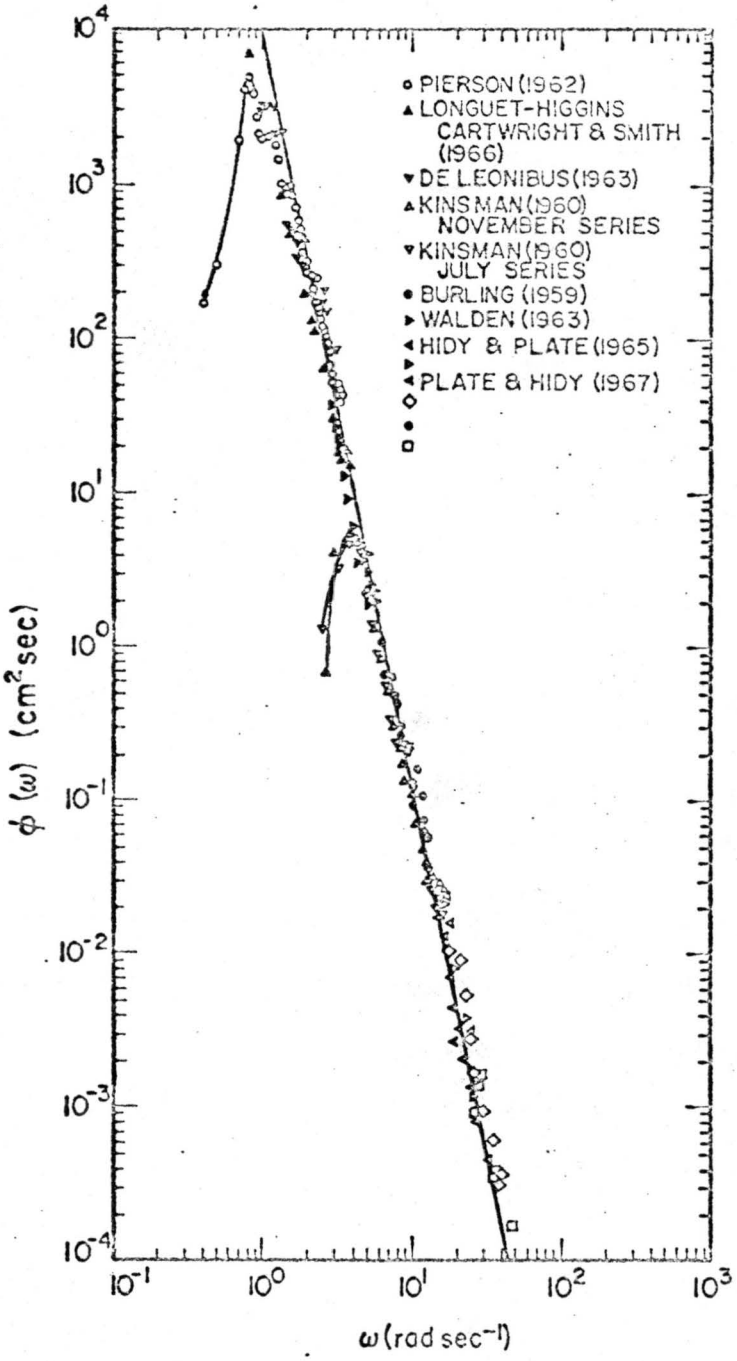

Fig. 3 A Comparison of Observed Wave Spectra with Geophysical Wave Spectra (from Hess, 1968)

Higgins (1952) this implies that the water surface undulations consist mainly of a train of waves of frequency ω_{max} whose amplitudes are subject to a random modulation. This model agrees well with observations both of water surface elevation recordings and of wave spectra. The wave of frequency ω_{max} shall be called the dominant wave, whose height is denoted by H_{max}.

b. The maximum growth of the dominant wave component is limited by the acceleration of gravity such that

$$a_{max} = \alpha g \tag{3}$$

where a_{max} is the maximum acceleration of the surface of the dominant wave, and α is a number which is smaller than 1. It will be shown that $\alpha \approx 0.3$ leads to an estimate which is consistent with the numerical factor of 0.0105 in Eq. 2.

Longuet-Higgins (1952) has shown that a Gaussian wave record which satisfies condition (a) above has wave heights, H which are Rayleigh distributed. Consequently, the mean value, $H^{(p)}$, of the pN highest of N waves is a constant multiple of the mean wave height $\overline{H}$, or

$$\frac{H^{(p)}}{\overline{H}} = m \tag{4}$$

where m is a constant. Typical values of m are $m = 1.42$ for $p = 1/3$ and $m = 1.26$ for $p = 1/2$. Thus, if each wave is basically sinusoidal, then the average vertical acceleration of the water particles at the peak of the highest pN dominant waves is found to be equal to:

$$a_m = \frac{1}{2} \omega_{max}^2 H^{(p)} \tag{5}$$

Somewhat arbitrarily, it is assumed that the significant acceleration is that of the significant wave $H^{(1/3)}$. For a wave record whose water surface elevation is Gaussian (which is approximately true both for the laboratory and the field), there exists the following relation between mean wave height and variance of the water surface elevation (Collins, 1966):

$$8 \sigma^2 = \overline{H}^2 \tag{6}$$

with $m = 1.42$, the relationship between the acceleration of the significant wave $H^{(1/3)}$ and the variance σ^2 of the wave record is found as:

$$a_m^2 = 4\ \omega_{max}^4\ \sigma^2 \tag{7}$$

But according to assumption Eq. 3, this is also equal to $\alpha^2 g^2$, so that

$$\sigma^2 = \frac{\alpha^2 g^2}{4\ \omega_{max}^4} \quad . \tag{8}$$

We can eliminate σ^2 in Eq. 1 and let $\omega = \omega_{max}$. It is then seen from Fig. 2 that $S(\omega_{max}/\omega_{max}) = S(1) \simeq 0.5$ for a fully developed sea, and consequently:

$$\phi(\omega_{max}) = \frac{\sigma^2}{\omega_{max}}\ 0.5 = \frac{\alpha^2 g^2}{8\ \omega_{max}^5} \tag{9}$$

which is independent of the spectral shape except for the requirement of similarity. This result is now compared with Eq. 2 where ω is replaced with ω_{max}. One obtains:

$$\phi(\omega_{max}) = 1.05\ 10^{-2}\ g^2\ \omega_{max}^{-5} \quad . \tag{10}$$

Consequently, one finds

$$\alpha = 0.29 \tag{11}$$

which is somewhat lower than the limiting vertical acceleration of the Stokes wave, where $\alpha = 0.5$.

The reasoning leading to Eq. 10 is of consequence for the purpose of modeling. When conducting a model study, it is naturally desirable

to model the maximum forces that can occur. Waves with amplitudes exceeding that of the significant wave would presumably break, because their accelerations exceed the critical value αg. Therefore, waves at frequencies $\omega > \omega_{max}$ of larger amplitudes than that at ω_{max}, cannot occur in an equilibrium spectrum described by the similarity shape and by the relation between peak spectral density and the corresponding frequency expressed through Eq. 10. If larger waves are to occur they must therefore be of lower frequencies.

Equation 10 also implies that the waves that reach the limit of growth are subjected to continuous addition of energy through work done by the wind, so that the dominant wave remains at its maximum height. A spectrum of waves with a dominant wave consisting of swell from a far away, and perhaps long subsided storm, might still have the similarity shape of wind generated waves, but its maximum spectral density will be below that of Eq. 10. Consequently, the maximum possible spectral density for waves of frequency ω_{max} is given by Eq. 10, which therefore describes the envelope for all fully developed wave spectra.

Fully developed wave spectra are found in particular when wind of long duration is blowing, such as during hurricanes. An example is given by results of Collins (1966) which were obtained at two different times at two different off-shore fetches during an off-shore blowing wind. In Table 1 the peaks of the spectra calculated from Eq. 10 are compared with the peaks obtained by Collins. It is remarkable that the long fetch spectra are in exact agreement with Eq. 10, while the lower fetch data are below the saturation value given by Eq. 10. Many other data show the same behavior, as is evident from the data of Fig. 3.

TABLE 1. PEAK AMPLITUDES OF HURRICANE DORA DATA
(from Collins, 1966)

Case	f_{max} (Hz)	$\phi(f_{max})$ (observed) m^2-sec	$\phi(f_{max}) = 2\pi\phi(\omega_{max})$ (from Eq. 10) m^2-sec	Remarks
AI	0.35	0.130	0.124	Sept. 9, 64 Fetch 11 miles
AII	0.45	0.018	0.034	Sept. 9, 64 Fetch 1.7 "
BI	0.23	1.05	1.00	Sept.10, 64 Fetch 11 "
BII	0.27	0.2	0.45	Sept.10, 64 Fetch 1.7 "

We notice that the results of Eqs. 9 and 11 yield the important relationship between variance, σ^2 , and ω_{max}:

$$\sigma^2 = 2.1\ 10^{-2}\ g^2\ \omega_{max}^{-4} \quad . \tag{12}$$

Equation 12 shows that the scale of the amplitudes of the wave which must also scale the square root of the variance of the spectrum fixes the scale of the frequencies, so that it is not possible to adjust the two scales independently. If it is desired to model wave heights so that

$$\left(\frac{\sigma}{L}\right)_m = \left(\frac{\sigma}{L}\right)_p \tag{13}$$

then it follows that the frequencies must be related like:

$$\frac{\sigma_m}{\sigma_p} = \frac{L_m}{L_p} = \frac{\omega^2_{max\ p}}{\omega^2_{max\ m}} \quad . \tag{14}$$

Here, L is any characteristic length, the subscript m refers to the model, and the subscript p to the prototype. This condition is in accord with the requirements imposed on the wave length λ . If it is desired to have identical non-dimensional wave lengths, λ/L , for model and prototype, then it would be necessary to set

$$\frac{L_m}{L_p} = \frac{k_p}{k_m} = \frac{\lambda_m}{\lambda_p} \quad . \tag{15}$$

However, for gravity water waves, the frequency is related to the wave number, $k = 2\pi/\lambda$, by:

$$\omega^2 = g\ k\ \tanh\ kh \tag{16}$$

where h is the depth, as defined in Fig. 4, and thus:

$$\frac{\omega_p^2}{\omega_m^2} = \frac{k_p}{k_m} = \frac{L_m}{L_p} = \frac{h_m}{h_p} \tag{17}$$

in agreement with Eq. 14. Consequently, the use of a fully developed wave spectrum in the laboratory for simulating a fully developed wave spectrum for prototype conditions results in identical scale ratios of both wave heights and wave lengths, if the spectra are related by Eq. 14. The use of Eq. 14 thus leads to an undistorted geometrical scaling of the whole wave field. This result establishes the advantage of using wind generated waves in the laboratory for modeling wind generated waves in the field.

It is interesting to note that modeling according to Eq. 14 implies Froude number scaling, i.e.,

$$Fr = \left.\frac{u_{wave}}{\sqrt{gL}}\right|_m = \left.\frac{u_{wave}}{\sqrt{gL}}\right|_p \tag{18a}$$

where u_{wave} is a wave related velocity such as c_o, or the wave induced at some reference depth. For the latter, u_{wave} is proportional to $\sigma\omega$ for any frequency component and one obtains:

$$\frac{\omega_m \sigma_m}{\sqrt{gL_m}} = \frac{\omega_p \sigma_p}{\sqrt{gL_p}} \quad . \tag{19}$$

If σ is eliminated through Eq. 14, then Eq. 17 follows. Consequently, Froude number modeling according to Eq. 19, in conjunction with Eqs. 9 and 10, results in fully developed wind generated wave spectra in model and prototype which are geometrically similar with equal vertical and horizontal scales. Therefore, the model structures can be built to scale, and the complications which arise from distorted scales can be avoided. It should be mentioned that the definition of a modeling Froude number according to Eq. 19 is somewhat more stringent than is required for linear response of structures under the effect of a wave force. For such a system, the amplitude appears only in the load function and therefore need not be scaled properly because its effect can be included into the conversion factor which is used for calculating prototype response data from model data. Then the Froude number is more suitably defined by

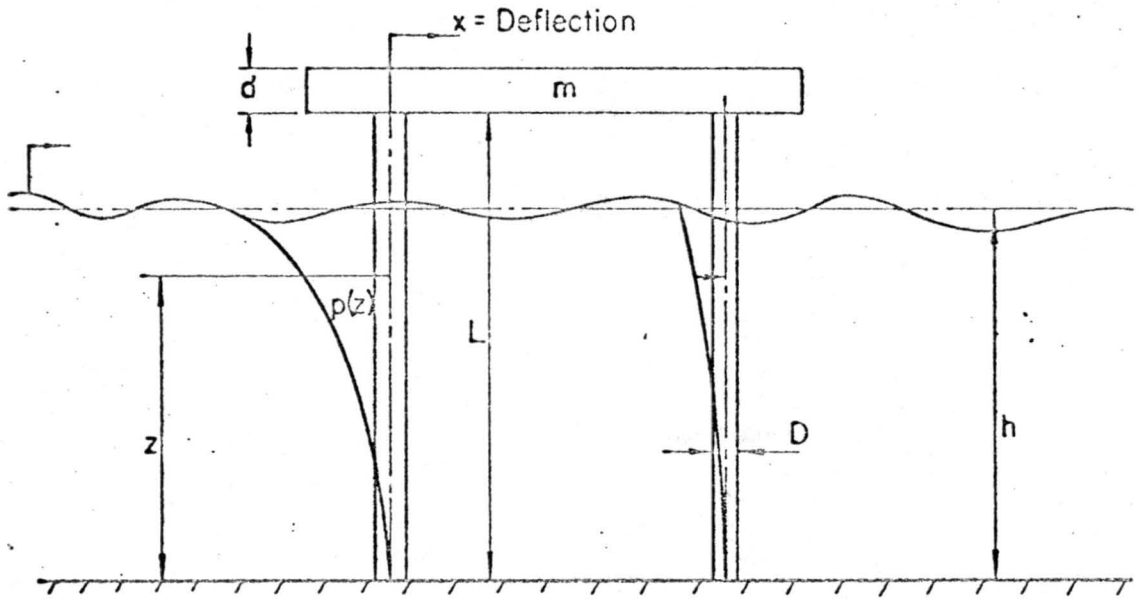

Fig. 4 Definition Sketch for Off--Shore Structure

$$Fr = \frac{c_o}{\sqrt{gL}} \qquad (20)$$

Since c_o is independent of the vertical scale of the wave motion, this modeling criterion only suffices to satisfy Eq. 15, but not Eq. 13.

In applying Eq. 10 to laboratory modeling, it is required that some value of the height of the significant wave is known which can be expected under prototype conditions at the position where the structure is to be constructed. How this wave height can be found shall not be discussed here. If it is known, then the variance of the water surface follows from Eqs. 4 and 6, the peak frequency, ω_{max}, from Eqs. 8 and 11, and the spectral peak from Eqs. 9 and 11. The spectrum can then be constructed with variance σ^2, ω_{max}, and the similarity spectrum of Fig. 2. After choosing a suitable length scale, the model spectrum can be obtained by reducing the variances of the water surface and the frequencies according to Eq. 14. It remains to show under what conditions it will be possible to obtain a scaled dynamic response of the structure.

Modeling of Structures Subjected to Wave Forces

When a linear structure is excited by a random dynamic load whose stationary spectrum is $\phi_L(\omega)$, it is well known that the deflection spectrum $\phi_x(\omega)$ of a characteristic point on the structure can be expressed by

$$K^2 \phi_x(\omega) = \left| H(\omega) \right|^2 \phi_L(\omega) \quad . \qquad (21)$$

where K is the spring constant of the support legs and H is a transfer function. Multiplication of the deflection spectrum by the square of the spring constant K of the support legs signifies that we assume the structure to be so stiff that deflections are within the range of validity of Hooke's law. Then the spring constant is a multiplier whose magnitude must be known. It is to be chosen according to dynamic similarity of the structural response.

The function $H(\omega)$ of Eq. 20 is the transfer function of the structure which establishes the dynamic response of the structure under the effect of the load spectrum. In our notation, it is a dimensionless

function whose value at zero frequency must be one, to correspond to the case of static loading. The simplest structure, such as shown in Fig. 4, consists of one or more cylindrical supports which are clamped to some degree into the ground and into the working platform. The transfer function of each of these cylinders is then given by that of a simple second order system:

$$\left|H(\omega)\right|^2 = \frac{1}{\left(1 - \frac{\omega^2}{\omega_n^2}\right)^2 + \left(2\zeta \frac{\omega}{\omega_n}\right)^2} \tag{22}$$

which is valid for the dominant first vibrational mode, whose natural frequency is equal to ω_n . The coefficient ζ is the relative damping factor. It is determined almost completely by the internal structural damping, while the natural frequency is given to:

$$\omega_n = \sqrt{\frac{K}{m}} \tag{23}$$

where m is the mass of the load on the single cylinder, and K is the spring constant:

$$K = \gamma \frac{3EI}{L^3} (1-\beta) \quad . \tag{24}$$

In this equation, E is the modulus of elasticity, I the moment of inertia, and L the length of the cylinders, as indicated in Fig. 4. The clamping coefficient γ corrects for the possibility of rotation of cylinder top and bottom. When the cylinder is clamped into the ground, and into the platform (i.e., the cylinder is one leg of a multilegged structure) so that the joints cannot rotate then $\gamma = 1$. A more flexible structure, resulting from only partial clamping in the ground or at the platform yields a smaller γ , while increased stiffness, as obtained for example by braces across the legs results in a larger value of γ . Evidently, for more complex structures a simple correction of the single cylinder spring constant does not suffice, and a suitable elastic model may be the only feasible alternative. The coefficient β is the reduction factor due to vertical loads, i.e.,

$$\beta = \frac{4WL^2}{\pi^2 EI} \qquad (25)$$

where W is the vertical load applied to the cylinder top. As long as β is significantly smaller than 1, a vertical load can be used to tune the structure, so that its natural frequency assumes the desired value.

For the multilegged structure as a whole, the transfer function is the same as that for the individual legs except for a modification factor which results from the time lag between the forces on different cylindrical legs. The phase shift may either lead to adding total forces on the structure or subtracting, and might even cancel depending on the distance between legs as related to wave length, and on the orientation of the structure. This effect has been discussed by Nath and Harleman (1968).

When the structure has many degrees of freedom and can vibrate at many different eigen modes, the structural response of a particular point on the structure is difficult to determine. However, a good first approximation may be made with a modal analysis wherein the following assumptions are made:

1. Viscous damping coefficients exist for each mode which are proportional to either the modal mass or the modal stiffness.

2. The phase relationships between modes are disregarded.

3. The cross-influences between modal responses have negligible effect on the response spectra.

Under these conditions the response spectrum is constructed from a linear summation of the response spectrum for each mode (Hurty and Rubinstein (1964)). In the following presentation the index i stands for the direction (either displacement or rotation) of the vibration and the index j for the modal order. Then the spectrum of the structural response, x, considering n modes, is:

$$\phi_{xi}(\omega) = \sum_{j=1}^{n} \phi_{xij}(\omega) \qquad (26)$$

and

$$\phi_{xij}(\omega) = A_{ij}(\omega) \left| H_j(\omega) \right|^2 \phi_L(\omega) \tag{27}$$

where:

$$\left| H_j(\omega) \right|^2 = \frac{1}{\left(1 - \frac{\omega^2}{\omega_{ij}^2} \right)^2 + \left(2\zeta_{ij} \frac{\omega}{\omega_{ij}} \right)^2} \tag{28}$$

is the transfer function of the j-th mode with eigen frequency ω_{ij} and damping factor ζ_{ij} in the i direction, and $A_{ij}(\omega)$ is a function embodying a generalized coordinate system and the relative participation from each mode due to modal shape and effective mass.

In most cases only the first few modes need to be considered. For ocean platforms in deep water, for example, it is possible that only the first mode is important and one probably never needs to consider modes beyond the fourth because the larger modal frequencies are usually much higher than any wave frequencies in the wave spectrum.

In a model study, the effects of structural complications and intramodal coupling on the transfer function may possibly be determined experimentally. We notice that for the transfer function to be modeled in the laboratory, it shall have to meet the following requirements:

1. Model and prototype must be geometrically similar, and must be scaled such that the length scales of the wave motion are identical to the scale of the geometry of the structure. In this manner, interference effects due to loads on different individual legs and other structural elements are accounted for.

2. Dimensionless (or relative) damping coefficients of model and prototype associated with each mode must be identical. This requirement is not met easily. It is probably suitable to use a damping coefficient based on experience and correct the damping of the model structure by an external arrangement of dashpots.

3. The natural frequencies of model and prototype must be chosen such that ω/ω_n is identical in model and prototype. This must be interpreted as requiring that the ratio of the ω_{max} of the peak of the load spectrum to the natural frequency of the structure, ω_n, is the same, or

$$\left(\frac{\omega_{max}}{\omega_n}\right)_{model} = \left(\frac{\omega_{max}}{\omega_n}\right)_{prototype} . \tag{29a}$$

It is evident, that in modeling a multi-degree of freedom structure, one must maintain:

$$\left(\frac{\omega_{max}}{\omega_{ij}}\right)_{model} = \left(\frac{\omega_{max}}{\omega_{ij}}\right)_{prototype} \tag{29b}$$

for all modes of importance.

Evidently, the preceding requirements imply that the output spectrum, as well as the input spectrum, is similar in model and prototype. The modeling requirement expressed by Eq. 29 implies simultaneous equality of both Froude number and Cauchy number in model and prototype. Generally speaking, the Cauchy number is defined as

$$C_a = \frac{u_W}{u_E} \tag{30}$$

where a wave reference velocity might be $u_W = \sigma\omega_{max}$, while the reference elastic velocity u_E usually is the speed of sound E/ρ. However, in the case of bending deformation of the structure, it appears to be more rational to use an elastic velocity $u_E = L\omega_n$, so that

$$C_a = \frac{\omega_{max}}{\omega_n}\frac{\sigma}{L} \tag{31}$$

for similar geometrics, Cauchy number similarity for model and prototype requires that Eq. 29 be satisfied. This equality together with Froude number equality can be met, however, only if the elastic properties are suitably adjusted. By using the definition of the natural frequency, Eq. 23, in conjunction with Eqs. 24, 14 and 30, it is seen that

$$\alpha \frac{E_m \rho_p}{E_p \rho_m} = \frac{L_m}{L_p} \tag{32}$$

when ρ_p and ρ_m are the bulk densities of the loads on the cylinder for prototype and model, respectively. The factor α, given by

$$\alpha = \frac{\gamma_m (1 - \beta_m) I_m L_p^4}{\gamma_p (1 - \beta_p) I_p L_m^4} \tag{33}$$

reduces to one if exact geometric similarity of the model and prototype support structures exist, and if the damping conditions are identical. A factor $\alpha = 1$ is, of course, not necessary. For example, instead of the thin-walled cylinders used for the legs of prototype structures, we might prefer to use solid legs in the model.

The result given by Eq. 31 can be derived more formally by the methods of inspectional analysis, as was evidently done by LeMehaute (1966). It gives a means of obtaining, by suitably adjusting α, E_m and ρ_m, the dynamically correct response of the structure to wave forces, provided that the load spectrum is also modeled properly.

The load spectrum is not directly proportional to the wave spectrum, but it is related to it. Under some conditions, a linear relation exists between load spectrum and wave spectrum

$$\phi_L(\omega) = G^2(\omega) \phi_\eta(\omega) \tag{34}$$

where $G(\omega)$ is a conversion factor, which depends on ω as well as many other factors.

Generally speaking, the function $G(\omega)$ is nonlinear and becomes dependent on the Reynolds number. It is found by integrating the contributions to the total deflection of the local load contributions $p(z)$ over the length of the submerged part of the structure. Below the water surface, the local load is described approximately by the Morrison equation:

$$p(z) = C_I \rho A a(z) + C_D \rho \frac{D}{2} |u(z)| u(z) \qquad (35)$$

where A is the cross-sectional area and D the diameter of the cylinder, ρ the fluid density, $u(z)$ and $a(z)$ are the velocity and the acceleration, respectively, of the fluid at the depth z. C_I is the coefficient of inertia which embodies both the contribution of virtual mass and of resultant unsteady pressure forces on the cylinder. For an infinitely long cylinder, its value is equal to 2. For a finite length cylinder subjected to wave forces which vary with depth h, C_I may vary with depth (Pierson and Holmes (1965)) and with the ratio of $2\pi h/D$ (Paape and Breusers (1966)). It is possible that the requirement of geometric similarity of model and prototype suffices for identity of C_I in both cases. Certainly, geometric similarity does permit to keep the ratio $2\pi h/D$ constant.

The drag coefficient C_D is more difficult to model properly. In principle, it depends on the local Reynolds number, and it is well known that Reynolds number scaling is incompatible with Froude number scaling. Unfortunately, very little is known about C_D in a wave situation, and for modeling purposes one has to make an assumption. One possibility is to artifically roughen the cylinders so that their effective Reynolds number is increased. It is well known that for large effective Reynolds numbers, the drag coefficient of an infinitely long cylinder becomes constant. Similar results might be expected for the wave case.

Fortunately, for deep water waves the effect of the drag appears to be small compared to that of the inertia, as was shown by Nath and Harleman (1967). Under this condition, the relation for the conversion factor $G(\omega)$ becomes:

$$G(\omega) = \rho C_I A \frac{B}{k} \frac{\omega^2}{2} \frac{1}{\tanh kh} \qquad (36)$$

when the assumption is made that C_I is constant over the height of the cylinder. B is a non-dimensional function:

$$B(kh) = \int_0^{kh} \frac{\cosh kz \left(1 - \cos \frac{\pi z}{2L}\right) d(kz)}{\cosh kh} \qquad (37)$$

By using $\omega^2 = gk \tanh kh$, it is seen that

$$G(\omega) = \rho C_I A \frac{g}{2} B(kh) \tag{38}$$

Since B is the same in model and prototype, geometric similarity is sufficient to scale $G(\omega)$ properly.

For shallow water, the inertia coefficient might be small as compared to the effective drag coefficient. Under these circumstances, it has been shown by Borgman (1967) that the leading term of a series expansion of the nonlinear drag term in the Morrison equation is still approximately linear. That is, the drag component is proportional to the drag coefficient times a slightly to moderately nonlinear multiplication factor. Even though Borgman's results have not been subjected to extensive experimental verification, it appears that, with exception of the drag coefficient itself, scaling of the geometry would scale the multiplication factor of the nonlinear drag in the Morrison equation.

Modeling of Structures Subjected to Wind Forces

The wind blowing over the water surface apart from generating the waves will affect the off-shore structure in three ways. A constant wind of long duration will set up a static load on the submerged support structure as a result of the drag of the wind induced water current. Since the drag is concentrated near the surface, the resulting static deflection might be of appreciable magnitude, even though the velocities are generally small (of the order of 3% of the reference wind speed). The second effect is the static load due to the mean wind velocity. This force is given by the drag exerted on the structure, and is equal to

$$F_A = C_{D_A} \frac{1}{2} \rho_A (\bar{u}_A^2)_{avg} \cdot \frac{DL}{2} \tag{39}$$

where C_{D_A} is the drag coefficient, the avg. subscript indicates an average with respect to height, $\bar{u}_A$ is the local temporal mean velocity and L is some length parameter of the structure. The subscript A refers to the air motion. Recent laboratory evidence indicates that the wind load on the exposed portions of the support legs should be treated separately from the remainder of the structure. This and other effects due to wind loading will be published in a paper by Aiston and Nath, which is now being prepared. The third effect is caused by the dynamic loading due to turbulence in the air.

Not enough is known at this time about the current induced load. Laboratory tests and some theoretical considerations (Plate, to be published) show that the surface velocity is proportional to the shear velocity

$$u_* = \sqrt{\frac{\tau_{ws}}{\rho_A}} \tag{40}$$

where τ_{ws} is the water surface shear stress exerted by the wind. It is also, on infinitely deep water, proportional to the fetch, and thus must be regarded as unknown for the prototype.

The mean velocity drag expressed by Eq. 39 is mostly the drag which is exerted on the superstructure. As long as the superstructure consists mainly of a rectangular platform, its drag coefficient is determined by the sharp edges on top and bottom of the platform and depends only on the platform geometry. At high winds, similarity of platform geometry thus insures identity of drag coefficients.

The velocity $\overline{u}_A(z)$ depends on the elevation above the water surface. Again the shape of the platform simplifies modeling as compared with modeling over land (see Davenport (1967), Plate and Quarishi (1965) for two slightly different methods of modeling the wind profile over land). The velocity can be assumed constant and equal to that found at the scaled height of the platform above the water under prototype conditions. If the wind velocity is given as part of the site specifications, similarity of wind forces can be obtained by geometric similarity and equality of wind velocity at the elevation of the platform's center of gravity above the water surface.

An uncertainty exists in the specification of ρ_A for model and prototype. It should be a density based on the mixture of air and water spray which is blown against the structure. No reasonable estimate can at present be given for the added forces resulting from the presence of spray. We only know that the laboratory wind will, at the high speeds required, also contain a large amount of spray. An investigation of the spray load seems to be in order, but has to our knowledge not yet been performed.

The dynamic load due to the wind on the structure is of much greater consequence, since in some cases it might add to the dynamic loads already present from the waves. Directly coupled to the waves there is a dynamic load which results from wave induced velocity fluctuations. The decrease of these velocity fluctuations with height is also scaled by geometric scaling so that in intensity and frequency these air waves will be modeled approximately by the modeling requirements given above. Actually, the laboratory waves may induce a fluctuation in the air flow which is smaller than that found over ocean waves, because in the laboratory separation occurs at the wave crests, which may not be, but probably is, the case in the ocean. However, these air loads are usually very small and well hidden in the much stronger

turbulence which exists over the wavy water surface. They will therefore be of any consequence only if the natural frequency of the structure's first mode is in the neighborhood of the spectral peak in the wave spectrum--a condition which obviously has to be avoided.

Forces due to air turbulence are generally small. However, since air turbulence spectra have their peaks at larger frequencies than wave spectra, and thus closer to the eigen-frequencies of the structure, their effect might be appreciable.

The scaling of dynamic loading due to turbulence has been investigated by Davenport (1966). He gives some results which indicate that the frequencies ω_o of the large eddies of the turbulent flow are roughly scaled by the geometric scale factor,

$$\omega_o = \frac{\bar{u}_A}{L} \tag{41}$$

Consequently, the turbulent frequencies in model and prototype must be related by:

$$\frac{\omega_{om}}{\omega_{op}} = \frac{\bar{u}_{Am}}{\bar{u}_{Ap}} \frac{L_p}{L_m} \tag{42}$$

which is compatible with the modeling criteria of Eq. 17 only if

$$\frac{\bar{u}_m}{\bar{u}_p} = \left(\frac{L_m}{L_p}\right)^{1/2} \tag{43}$$

The same result is obtained if the forces due to eddy shedding from the bluff edges of the platform are considered. It is well known that for large enough Reynolds numbers the Strouhal number of the eddies shed, by the structure will be the same in model and prototype. Some values of interest for off-shore structures are the square, long cylinder tests of Vickery (1966), who found typically for a square cylinder

$$S = \frac{\omega D}{2\pi\bar{u}} = 0.12 \tag{44}$$

where S is the Strouhal number of the shed eddies and D is the thickness of the square cylinder. It is seen that identical Strouhal numbers for model and prototype lead again to the scaling requirements of Eqs. 42 and 43.

In conclusion, we find that aerodynamic modeling of the dynamic loads due to turbulence, is possible. However, it will be difficult to obtain model wind generated waves of sufficient amplitude at the wind velocities required by Eq. 43. This will be illustrated in the next section. It will probably be found more feasible to study separately the effects of wind loads and wave loads, for example, by shielding the superstructure from direct winds during the tests for response to waves and by shielding the submerged structure from waves during the tests for wind forces, and by assuming superposition of wind and wave responses.

Procedure of Modeling

The design information which must be available for modeling are the significant wave $H^{(1/3)}$ of the fully developed design spectrum, the maximum wind at the platform height or preferably the design wind velocity profile, the shape of the structure and its structural loads and elastic properties. In particular, we require the modulus of elasticity E_p of the prototype legs, their diameter D_p, length L_p and moment of inertia I_p, and the weight of the superstructure (we assume again that β is so small as to be negligible). We also need to know the depth of flow.

The modeling procedure is best illustrated by means of an example.

Let the depth of water be 400 feet in which a structure with four support legs is constructed. Let the diameter of the circular legs be 20 feet and let the platform be, say, 200 feet square in plan and about 40 feet thick. The platform is about 40 feet above the mean water surface level. Let us presume that we have a wind-wave tunnel such that a 4 foot water depth is obtainable, so a scale ratio of 1:100 will be used. The modeling of the wave spectrum, the structure, and the wind should proceed about as indicated below.

a) Modeling the wave spectrum

The structure is supposed to be subjected to a wave spectrum with a significant wave height of 8 meters, at a speed at platform height of 30 m/sec. This yields a standard deviation $\sigma_p = 2m$ according to Eqs. 4 and 6. From Eq. 8, $\omega_{max\,p} = 0.84$ rad/sec and from Eq. 10 $\phi_p(\omega_{max}) = 2.4$ m^2-sec. With these values, the corresponding prototype spectrum is found from the similarity form of Fig. 2.

The standard deviation of the model spectrum is now obtained from Eq. 14 and is 2 cm. The frequency $\omega_{max\,m}$ is found from the same equation to be 8.75 rad/sec. The corresponding height of the significant wave $H^{1/3}$ follows from Eqs. 4 and 6 to 8 cm. A fully developed wave

spectrum with peak characteristics as given can be obtained in the laboratory at a fetch and wind speed which can, to a first approximation, be determined from the fetch graph of Wiegel (1964). It appears that for high wind speeds laboratory data yield the following equation representing a portion of the fetch graph:

$$H^{(1/3)} = \frac{0.003}{\sqrt{g}} \bar{u} F^{1/2} \qquad (45)$$

With a model wind velocity = 1/2 prototype wind velocity - 15 m/sec, (to avoid excessive blow-off of crest) it follows that F = 15.5 m, which can be obtained conveniently in wind-wave tanks of existing designs.

If it is devised to obtain equality of Strouhal numbers of the air flow in addition to the wave conditions, then the wind in the model must be reduced, according to Eq. 43, to 3 m/sec. It is doubtful that Eq. 45 is valid for such a low air velocity, but if, for the sake of illustration, its validity is assumed it follows that a fetch of 775 m is required for modeling--well outside of any reasonable size of a laboratory facility.

b) Modeling the structure

The prototype structure is probably constructed of steel, so that $E_p = 29 \times 10^6$ psi. Let us say that the period of the first mode of vibration is 5 seconds so that $\omega_{np} = 1.25$ rad/sec which is obtained by analysis using design information of mass distribution, etc. Here we will only consider the first mode, or fundamental frequency.

The size of the model at a scale ratio of 1:100 will be: leg diameter of 0.2 feet, a platform of 2.0 feet square in plan and 0.4 feet thick. The platform is about 0.4 feet above the still water surface. Let us assume that a good grade of plastic is used for the model structural material, so that $E_m = 0.5 \times 10^6$ psi. The model should be constructed with the proper cross-sections and mass distribution such that $\omega_{nm} = 12.5$ rad/sec. from Eq. 29a. As is seen from Eq. 32, for the given conditions one must obtain $\alpha \rho_p/\rho_m = 0.58$. Since α is likely to be larger than 1, the easiest way of obtaining the desired natural frequency is by increasing the weight of the platform.

Acknowledgments

Financial support for this study has been provided by the National Science Foundation under Grant No. GK 188. P. C. Chang kindly made Fig. 1 available, which will appear in his Ph.D. Dissertation at Colorado State University.

REFERENCES

1. Borgman, L. E., (1967), "Spectral analysis of ocean wave forces on piling," Proc. ASCE, Vol. 93, Journal Waterways and Harbors Div., p. 129.

2. Collins, J., (1966), "Wave statistics from Hurricane Dora near Panama City, Florida," Proc. ASCE Conference on Coastal Engineering, Santa Barbara, p. 461.

3. Davenport, A. G., (1967), "Gust loading factors," Proc. ASCE, Vol. 93, Journal Structural Div., ST 3, P. 11.

4. Hurty, W. C. and M. F. Rubinstein, (1965), "Dynamics of Structures," Prentice-Hall, Englewood Cliffs, New Jersey.

5. Hess, G. D., (1968), "Turbulent air flow over small water waves," Ph. D. Dissertation, Department of Meteorology, University of Washington, Seattle, Washington.

6. Hidy, G. M., and E. J. Plate, (1965), "The frequency spectra of wind generated waves," Physics of Fluids, p. 1387.

7. Le Mehaute, B., (1965), "On Cauchy-Froude similitude," Proc. ASCE Conference on Coastal Engineering, Santa Barbara, p. 327.

8. Longuet-Higgins, (1952), "On the statistical distribution of the heights of sea waves," Journal of Marine Research, Vol. 11, p. 245.

9. Nath, J. H., and D. R. F. Harleman, (1967), "The dynamics of fixed towers in deep water random waves," Proc. of the Conference, "Civil Engineering in the Oceans," ASCE, San Francisco, California, p. 99.

10. Paape, A. and H. N. C. Breusers (1966), "The influence of pile dimensions on forces exerted by waves," Delft Hydraulics Laboratory, Publication No. 41, Delft, Nederland.

11. Phillips, O. M., (1958), "The frequency spectra of wind generated waves," Journal of Fluid Mechanics, Vol. 4, p. 426.

12. Pierson, W. J., and P. Holmes, (1965), "Irregular wave forces on a pile," Proc. ASCE, Vol. 91, Journal Waterways and Harbors Div., WW 4, p. 1.

13. Pierson, W. J., and Moskowitz, L., (1964), "A proposed spectral form for fully developed wind seas based on the similarity theory of Kitaigorodskii," Journal of Geophysical Research, Vol. 69, No. 24, p. 5181.

14. Plate, E. J., P. Chang and G. M Hidy, (1968), "Experiments on the generation of small water waves by wind," Journal of Fluid Mechanics, (to be published).

15. Plate, E. J., and A. A. Quaraishi, (1965), "Modeling of velocity distributions inside and above tall crops," Journal of Appl. Meteorology, Vol. 3, p. 400.

16. Vickery, B. J., (1966), "Fluctuating lift and drag on a long cylinder of square cross section in a smooth and in a turbulent stream," Journal of Fluid Mechanics, Vol. 25, p. 481.

17. Wiegel, R. L., (1964), "Oceanographical Engineering," Prentice-Hall, Englewood Cliffs, New Jersey.

LIST OF FIGURES